

Higher-order triangular and tetrahedral finite elements with mass lumping for solving the wave equation

M. J. S. CHIN-JOE-KONG¹, W. A. MULDER^{2*} and M. VAN VELDHUIZEN¹

¹*Vrije Universiteit, Faculty of Mathematics and Computer Sciences, Amsterdam, The Netherlands*

²*Shell International Exploration and Production B.V., Postbus 60, 2280 AB Rijswijk, The Netherlands*

e-mail: w.a.mulder@siep.shell.com

Received 3 December 1997; accepted in revised form 28 October 1998

Abstract. The higher-order finite-element scheme with mass lumping for triangles and tetrahedra is an efficient method for solving the wave equation. A number of lower-order elements have already been found. Here the search for elements of higher order is continued.

Elements are constructed in a systematic manner. The nodes are chosen in a symmetric way. Integration rules must be exact up to a certain degree to maintain an overall accuracy that is the same as without mass lumping. First, for given integration degrees, consistent rule structures are derived for which integration formulas are likely to exist. Then, as each rule structure corresponds to a potential element of certain order, the position of element nodes and the integration weights can be found by solving the related system of nonlinear equations.

With this systematic approach, a number of new sixth-order triangular elements and a new fourth-order tetrahedral element have been found.

Key words: finite elements, mass lumping, numerical quadrature, wave equation, acoustics, seismics.

1. Introduction

Computers are becoming sufficiently powerful for direct simulation of wave propagation through a portion of the earth or another type of solid. The finite-difference method (FDM) is a popular numerical technique because it is relatively easy to implement and allows for straightforward parallelisation. It is, however, difficult to model rugged topography and irregular boundaries on regular cartesian grids with higher-order finite differences. Also, the FDM becomes less accurate near abrupt changes in the velocity model.

Finite elements for triangles and tetrahedra are better suited to model rugged topography and sharp contrasts in velocity models, because element boundaries can be fitted to the model boundaries and to sharp interfaces in the model. The finite-element method (FEM) in its original form requires the solution of a large sparse linear system of equations, which makes the method costly. This cost can be avoided by mass lumping, a technique that replaces the large linear system by a diagonal matrix. New elements must be constructed to maintain sufficient numerical accuracy after mass lumping [1].

One question is whether or not the superior accuracy of the FEM allows for a reduction of the number of degrees of freedom that is large enough to balance its higher cost. Higher-order finite elements with mass lumping can be used for solving the wave equation. This approach was used for two-dimensional triangulations in [2–5]. In [5] it was shown that the same approach can be extended to tetrahedra. It was also shown by a comparison on a simple two-

* Author for correspondence.

dimensional reflection problem that the higher-order FEM is more efficient than the FDM. A comparison between finite-element schemes of various orders revealed that the higher-order approximations are more efficient than the lower orders. This motivates the search for elements of still higher order.

So far, elements up to fifth order for triangles and third order for tetrahedra have been found (in one space dimension, the Gauss–Lobatto points will provide suitable mass-lumped elements [6]). Here we continue the search for higher-order elements in a systematic manner, using the theory on consistency conditions for symmetric integration rules [7–9]. Mass lumping without loss of accuracy is equivalent to numerical integration with certain weights on the element nodes. The numerical integration is accurate to a certain order if all polynomials up to a given degree are integrated exactly. This leads to a system of equations that is linear in the integration weights and polynomial in the parameters describing the node positions. Because this nonlinear system is, in general, difficult to solve, it helps to have conditions that guarantee the existence of a solution. The consistency conditions ensure that there is a sufficient number of nodes and node parameters to integrate the polynomials exactly and that the number of equations does not exceed the number of unknowns. Although the conditions are neither necessary nor sufficient for general nonlinear systems, this approach turned out to be fruitful for the present problem.

In Section 2 some basic aspects of the FEM and the idea of mass lumping are briefly reviewed. Section 3 describes symmetric integration rules for the triangle and tetrahedron. Following the theory on consistency conditions, see [7–9] optimal rule structures are derived for which integration rules are likely to exist. The conditions are given explicitly for two and three dimensions in Appendix A. Section 4 describes the actual construction of finite elements. The search is limited to elements with polynomial basis functions that have a restriction to the edges of degree M . The vertices are required to be included as nodes, as are $M - 1$ symmetrically arranged nodes on the edges. The polynomials may be of higher degree in the interior. For tetrahedra, the polynomials should be uniquely defined on the faces, that is, the number of degrees of freedom should match the number of nodes. This includes the above requirements on the edges.

Section 5 compares the computational efficiency of a newly found sixth-order triangular element to that of lower orders, in order to see if the added complexity is more than balanced by the improved accuracy. Numerical experiments are performed for a simple two-dimensional seismic reflection problem. A comparison between various temporal orders is included as well.

A seismic application for a hilly area is presented in Section 6. The main results of this paper are summarised in Section 7.

2. Some aspects of the FEM

Consider the wave equation in $n = 2$ and 3 dimensions

$$\frac{1}{c(\mathbf{x})^2} \frac{\partial^2 u(t, \mathbf{x})}{\partial t^2} = \Delta u(t, \mathbf{x}) + f(t, \mathbf{x}), \quad (1)$$

on a domain $\Omega \subset \mathbb{R}^n$ with initial conditions $u(0, \mathbf{x}) = (\partial u / \partial t)(0, \mathbf{x}) = 0$ and, for simplicity, homogeneous Dirichlet boundary conditions. The weak form of this equation is given by

$$\int_{\Omega} \frac{1}{c(\mathbf{x})^2} \frac{\partial^2 u(t, \mathbf{x})}{\partial t^2} v(\mathbf{x}) d\Omega$$

$$= - \int_{\Omega} \nabla u(t, \mathbf{x}) \cdot \nabla v(\mathbf{x}) \, d\Omega + \int_{\Omega} f(t, \mathbf{x}) v(\mathbf{x}) \, d\Omega \quad (2)$$

for all test functions $v \in H_0^1(\Omega)$.

A finite-element discretisation is obtained by subdividing the domain Ω into a finite number of regions \mathbf{T}^j , $j = 1, \dots, N$, in each of which a number of nodes is chosen. For each node $\mathbf{x}^{(i)}$ in \mathbf{T}^j a shape function ϕ_i^j is defined as a polynomial satisfying the following:

- ϕ_i^j takes the value 1 at $\mathbf{x}^{(i)}$ and vanishes in all the other nodes in \mathbf{T}^j : $\phi_i^j(\mathbf{x}^{(k)}) = \delta_{ik}$,
- ϕ_i^j has a prescribed behaviour on each subregion, depending on the number of nodes,
- the shape functions are continuous across neighbouring elements.

The finite-element space $V^h \subset H_0^1(\Omega)$ is defined as a linear span of basic functions. Elements of V^h are called trial functions. The finite-element approximation is a function of V^h satisfying (2) and is said to be conforming if it is continuous across the element boundaries.

The finite-element semi-discretisation of (2) is of the following form

$$\mathbf{M}^h \frac{\partial^2 u^h(t)}{\partial t^2} + \mathbf{R}^h u^h(t) = \mathbf{F}^h, \quad (3)$$

where \mathbf{M}^h and \mathbf{R}^h are the mass and stiffness matrix, respectively, and \mathbf{F}^h is the discretisation of the source term. A finite-difference scheme can be used for the time-discretisation. A second-order scheme is

$$\mathbf{M}^h \frac{u_{n+1} - 2u_n + u_{n-1}}{(\Delta t)^2} + \mathbf{R}^h u_n = \mathbf{F}^h. \quad (4)$$

Higher orders in time can also be used (see [2–5, 10]). The solution of (4) for u_{n+1} requires the inverse of the mass matrix, which is large and sparse. Inversion of such a matrix requires a substantial computational effort. Following [1–4], the cost involved is avoided by the application of mass lumping: the mass matrix is replaced by a diagonal matrix.

In two-dimensions, the element mass matrix corresponding to the triangle \mathbf{T}^j is given by

$$\frac{1}{c_j^2} J_j m^j, \quad m_{kl}^j = \int_{\mathbf{T}} \phi_k^j(\mathbf{t}^j(\xi, \eta)) \phi_l^j(\mathbf{t}^j(\xi, \eta)) \, d\xi \, d\eta, \quad (5)$$

where \mathbf{T} is the standard triangle with vertices $(0, 0)$, $(1, 0)$, $(0, 1)$ and $J_j = (x_2 - x_1)(y_3 - y_1) - (x_3 - x_1)(y_2 - y_1)$ is the Jacobian of \mathbf{t}^j , a linear transformation which maps \mathbf{T} onto \mathbf{T}^j . When applying a numerical integration rule with abscissae ξ_i and η_i and weights w_i , we obtain an approximate element mass matrix, given by

$$\tilde{m}_{kl}^j = \sum_{i=1}^n w_i \phi_k^j(\mathbf{t}^j(\xi_i, \eta_i)) \phi_l^j(\mathbf{t}^j(\xi_i, \eta_i)). \quad (6)$$

By construction, the nodes of the integration rule are the nodes of the element, hence

$$\phi_k^j(\mathbf{t}^j(\xi_i, \eta_i)) = \delta_{ki} \quad \text{and} \quad \phi_l^j(\mathbf{t}^j(\xi_i, \eta_i)) = \delta_{li}.$$

It follows that

$$\tilde{m}_{kl}^j = \delta_{kl} w_k,$$

showing that the approximate element mass matrix is diagonal with diagonal elements equal to the integration weights.

A necessary condition for mass lumping is that the integration weights do not vanish. Another condition involves the stability of the temporal discretisation (4), which leads to

$$0 \leq \tilde{\mathbf{M}}^{-1} \mathbf{R} \leq \text{Const.} \quad (7)$$

Here $\tilde{\mathbf{M}}$ is the lumped mass matrix and \mathbf{R} the stiffness matrix obtained by exact evaluation. The upper bound can be derived as follows. The z -transform in time can be expressed as $u_n = z^n u_0$. Let q be an eigenvalue of $\tilde{\mathbf{M}}^{-1} \mathbf{R}$. We obtain the equation $z - 2 + z^{-1} = -(\Delta t)^2 q$ from (3) by ignoring the source term \mathbf{F}^h . This equation has two roots with $|z| = 1$ for $0 \leq q \leq 4/(\Delta t)^2$, implying stability (and conservation of energy) if the eigenvalues all lie in this range. Eigenvalues outside this range will lead to instability ($|z| > 1$).

As \mathbf{R} is positive semi-definite, (7) is satisfied for nonnegative $\tilde{\mathbf{M}}$. Because all elements of $\tilde{\mathbf{M}}$ should be nonzero, $\tilde{\mathbf{M}}$ must be positive definite; in other words, the integration weights must be strictly positive.

The mass-lumped finite elements should obey the following requirements:

- (i) conformity,
- (ii) symmetric arrangement of nodes,
- (iii) positive integration weights,
- (iv) same order of accuracy as elements without mass lumping.

To obtain conformity, the search is restricted to elements that include the vertices as nodes. Also, the restriction of the shape functions to the edges should define a unique polynomial of degree $M \geq 1$. Among the integration rules that allow us to obey all these requirements, the ones with the fewest nodes are of interest for practical applications.

Note that some of the requirements may be relaxed: nonconforming elements of nonsymmetric choices of nodes may be of practical interest. These options have not been considered so far.

3. Integration-rule structures

The construction of integration rules of given degree starts with a choice of nodes in the standard element, a so-called rule structure. The requirement that the integration rules be exact for polynomial shape functions up to a certain degree leads to a system of equations that is linear in the integration weights and nonlinear (polynomial) in the parameters that describe the positions of the nodes. For low degrees, the system can be solved manually. A symbolic algebra package may provide answers for somewhat higher degrees, but, in general, a brute-force numerical approach appears to be the only option for higher-degree elements. In that case, it helps if the solvability of the system can be determined *a priori*.

With the approach of [7–9], rule structures can be selected for which integration rules are *likely* to exist. The requirement is that the number of linearly independent equations in the nonlinear system does not exceed the number of unknowns. This should also hold for subsystems that contain only a subset of the unknowns and are obtained by taking linear combinations of the equations. These requirements result in a set of inequalities that are referred to as consistency conditions. Although these conditions are necessary and sufficient for linear independence of the system, they are neither necessary nor sufficient for the existence and/or

uniqueness of solutions of the nonlinear system. However, they still provide a starting point for a systematic search.

The system of equations is derived from the requirement that all polynomials up to a certain degree should be integrated exactly. The symmetric arrangement of nodes allows for a reduction of the number of polynomials that have to be considered. This implies a reduction of the number of equations, as is reviewed in Section 3.1.

We obtain the first consistency condition by requiring that the total number of unknowns should be less than or equal to the total number of equations. The latter equals the dimension of the space of the reduced set of polynomials. Next, subsystems should be taken into account. These exist because some of the polynomials are integrated to zero by the quadrature rule on certain classes of nodes. This leads to the consideration of null spaces and provides additional inequalities. The resulting inequalities for a given degree of the integration are called consistency conditions (Section 3.2).

The next step is the solution of the set inequalities, which is an integer optimisation problem. Here this problem has been approached by simple enumeration. The result is a long list of rule structures (choice of nodes). Each rule structure corresponds to a nonlinear system of weights and node parameters, which still has to be solved (Section 4).

As already mentioned, the consistency conditions make it likely that a solution exists. Nonlinearities, however, may cause problems: consistent systems may fail to have solutions, and inconsistent systems may still have solutions due to peculiar degeneracies of the nonlinear terms. Nevertheless, this approach has allowed us to reproduce all known elements and a few new ones.

3.1. SIMPLICIALLY SYMMETRIC QUADRATURE FORMULAS

The n -dimensional simplex S_n is defined by

$$S_n = \left\{ \mathbf{x} \in \mathbb{R}^n \mid 0 \leq x_i \leq 1, \quad i = 1, \dots, n, \quad \sum_{i=1}^n x_i \leq 1 \right\}.$$

Two points $\mathbf{x} = (x_1, \dots, x_n)$ and $\mathbf{y} = (y_1, \dots, y_n)$ in S_n are said to be simplicially symmetric if $\tilde{\mathbf{x}} = (x_1, \dots, x_n, 1 - \sum_i x_i)$ can be obtained from $\tilde{\mathbf{y}} = (y_1, \dots, y_n, 1 - \sum_i y_i)$ by permutation of the coordinates of $\tilde{\mathbf{y}}$. This is an equivalence relation, and in any equivalence class there are at most $(n+1)!$ points.

Simplicially symmetric quadrature formulas, all of whose evaluation points lie in the n -simplex, assign the same weight to $\mathbf{x} = (x_1, \dots, x_n) \in S_n$ as they do to all points simplicially symmetric to \mathbf{x} . A basic simplex rule $J(\alpha)$, with $\alpha \in S_n$, is defined as a functional

$$J(\alpha) f = \sum_{\bar{\alpha} \sim \alpha} f(\bar{\alpha}), \tag{8}$$

the sum being over all points simplicially symmetric to α . A simplicially symmetric quadrature formula Q for S_n is a weighted sum of basic rules

$$Q(f) = \sum_{i=1}^N w_i J(\alpha^{(i)}) f, \tag{9}$$

where $\alpha^{(i)} = (\alpha_1^{(i)}, \dots, \alpha_n^{(i)})$.

Table 1. Basic integration rules for the triangle.

Class $[\mathbf{n}]$	Rule	$v[\mathbf{n}]$
[1]	$J(0, 0)$	3 vertices
[2]	$J(\frac{1}{2}, 0)$	3 midpoints of edges
[1, 1]	$J(\alpha, 0)$	6 interior points of edges
[3]	$J(\frac{1}{3}, \frac{1}{3})$	1 centre of triangle
[2, 1]	$J(\alpha, \alpha)$	3 interior points
[1, 1, 1]	$J(\alpha, \beta)$	6 interior points

Table 2. Basic integration rules for the tetrahedron.

Class $[\mathbf{n}]$	Rule	$v[\mathbf{n}]$
[1]	$J(0, 0, 0)$	4 vertices
[2]	$J(\frac{1}{2}, 0, 0)$	6 midpoints of edges
[1, 1]	$J(\alpha, 0, 0)$	12 interior points of edges
[3]	$J(\frac{1}{3}, \frac{1}{3}, 0)$	4 centres of faces
[2, 1]	$J(\alpha, \alpha, 0)$	12 interior points of faces
[1, 1, 1]	$J(\alpha, \beta, 0)$	24 interior points of faces
[4]	$J(\frac{1}{4}, \frac{1}{4}, \frac{1}{4})$	1 centre of tetrahedron
[3, 1]	$J(\alpha, \alpha, \alpha)$	4 interior points
[2, 2]	$J(\alpha, \alpha, \frac{1}{2} - \alpha)$	6 interior points
[2, 1, 1]	$J(\alpha, \alpha, \beta)$	12 interior points
[1, 1, 1, 1]	$J(\alpha, \beta, \gamma)$	24 interior points

Let $\mathbf{x} = (x_1, \dots, x_n) \in S_n$ and $x_{n+1} = 1 - \sum_{i=1}^n x_i$. If $(x_1, \dots, x_n, x_{n+1})$ has r nonvanishing coordinates of which k are distinct, $0 \leq k \leq r \leq n+1$, and the j th nonvanishing coordinate appears n_j times, $j = 1, \dots, k$, and $n_1 + \dots + n_k = r$, then the basic rule $J(\mathbf{x})$ is said to be of class $[n_1, \dots, n_k]$, abbreviated as $[\mathbf{n}]$, and it uses

$$v[\mathbf{n}] = \frac{(n+1)!}{n_1! n_2! \dots n_k! (n+1-r)!} \quad (10)$$

function evaluations.

In two dimensions, with the constraint $\sum_{i=1}^3 \alpha_i = 1$, there are 6 different classes of basic rules, see Table 1. The symmetry points of (α, α) lie on a median line through the centre and one vertex. The symmetry points of (α, β) lie between the edges and the median lines.

In three-dimensions, with the constraint $\sum_{i=1}^4 \alpha_i = 1$, there are 11 different classes of basic rules, see Table 2. The symmetry points $(\alpha, \alpha, 0)$ lie on the median lines of the faces and the points $(\alpha, \beta, 0)$ lie between these median lines and the edges. In class [3, 1] each point lies on a median line through the centre of the tetrahedron and one vertex. In classes [2, 2] and [2, 1, 1] each point lies on a median plane through the centre and two vertices. Points in class [1, 1, 1, 1], not lying on any median lines or planes, have arbitrary positions in the tetrahedron.

An integration rule Q is of polynomial degree d if it integrates all polynomials up to degree d exactly

$$Q(f) = I(f), \quad \forall f \in P_d, \quad (11)$$

where $I(f)$ is the exact integral. Such an equation for $f \in P_d$ will be referred to as a moment equation. Not all polynomials in P_d have to be considered, but only the subset P_d^n defined by the linear span of the monomials

$$x_1^{i_1} x_2^{i_2} \dots x_n^{i_n} (1 - x_1 - \dots - x_n)^{i_{n+1}},$$

$$i_1 = i_2 \geq i_3 \geq \dots \geq i_{n+1} \geq 0, \quad \sum_{j=1}^{n+1} i_j \leq d.$$

The following theorem is stated in [9] and will be used to construct the integration rules.

THEOREM 1. *Let Q be a simplicially symmetric integration rule. Then Q is a degree d approximation to the integral over the n -simples S_n if and only if*

$$Q(f) = \int_{S_n} f \, d\mathbf{x} \text{ for all } f \in P_d^n. \quad (12)$$

3.2. CONSISTENCY CONDITIONS

Preferred integration rules are those with as few integration points as possible and with a symmetric arrangement of modes. Additional requirements such as positive weights and conformity will be described in Section 4. Before the idea of consistency conditions is reviewed, some notation is introduced. Each symmetric integration formula Q has a structure, specified by rule structure parameters

$$K[\mathbf{n}] = \text{number of basic rules of class } [\mathbf{n}] \text{ in } Q.$$

A basic rule of class $[\mathbf{n}] = [n_1, \dots, n_k]$ on the n -simplex has k parameters associated with it: one integration weight and $k - 1$ parameters α_j , $j = 1, \dots, k - 1$; the parameter α_k is then equal to $1 - \sum_{j=1}^{k-1} \alpha_j$. The number of parameters in the basic rule of class $[\mathbf{n}]$ is denoted by $k[\mathbf{n}]$.

To assure that an integration rule can be of a given degree d , the numbers of basic rules of each type must satisfy certain consistency conditions. The basic requirement is that the number of equations produced by (12) does not exceed the number of unknowns. This translates into the condition that

$$\sum_{\text{all } [\mathbf{n}]} k[\mathbf{n}] K[\mathbf{n}] \geq \dim P_d^n.$$

Other trivial conditions are those that state that rules on nodes that do not have any parameters other than the integration weight, occur at most once. For the two-dimensional case, this implies that $K[1] \leq 1$, $K[2] \leq 1$, and $K[3] \leq 1$; in the three-dimensional case, there is an additional condition $K[4] \leq 1$.

Other consistency conditions for the rule structures are required because there may exist linear combinations of the equations defined by (12) in which some of the node parameters disappear. In these sub-systems, the number of equation may actually exceed the number of unknowns, which violates the basic requirement. To prevent this situation, additional inequalities of the form

$$\sum_{[\mathbf{n}]} k[\mathbf{n}] K[\mathbf{n}] \geq N_d \tag{13}$$

are required. To obtain a *complete* set of consistency conditions, the null spaces of the basic rules have to be taken into account. The right-hand side N_d in (13) indicates the dimension of an intersection of those null spaces.

The null space of rules of class $[\mathbf{n}]$ in P_d^n is the set of polynomials in P_d^n which are integrated to zero by all rules J of class $[\mathbf{n}]$, and is denoted by

$$M_d^n[\mathbf{n}] = \text{span}\{p \in P_d^n \mid Jp = 0 \ \forall J \in [\mathbf{n}]\}.$$

If N_d is the dimension of an intersection of null spaces of, say classes $[\mathbf{n}_{i_1}], \dots, [\mathbf{n}_{i_j}]$, then the sum in (13) is taken over all classes $[\mathbf{n}]$ but $[\mathbf{n}_{i_1}], \dots, [\mathbf{n}_{i_j}]$.

The determination of null spaces and corresponding inequalities is described in detail in [7]. Here the idea is only illustrated by an example. Consider the space $P_3^2 = \text{span}\{1, xy, xy(1 - x - y)\}$. Then it can easily be seen that

$$M_3^2[1] = \text{span}\{xy, xy(1 - x - y)\}, \quad M_3^2[2] = \text{span}\{xy - \frac{1}{12}, xy(1 - x - y)\}.$$

The intersection of these null spaces is obviously one-dimensional, namely $p = xy(1-x-y)$. This polynomial is also integrated to zero by the basic rule on nodes of class [1, 1], i.e., $p \in M_3^2[1, 1]$. The corresponding consistency condition is given by

$$K[3] + 2K[2, 1] + 3K[1, 1, 1] \geq 1.$$

This means that there should be at least one moment equation for which this polynomial p is not integrated to zero.

The resulting consistency conditions can be expressed as a set of linear inequalities of the form

$$\mathbf{A}\mathbf{K} \leq -\mathbf{r}(d),$$

where \mathbf{K} is the vector of rule structure parameters, using the same order as followed in Tables 1 and 2, so $K_1 = K[1]$, $K_2 = K[2]$, $K_3 = K[1, 1]$, etc. The matrix \mathbf{A} containing the numbers $k[\mathbf{n}]$, and the column vector $\mathbf{r}(d)$ of null space dimensions are given in Appendix A. The null space dimensions $\mathbf{r}(d)$ are tabulated up to degree $d = 14$ for the 2-simplex and up to degree $d = 12$ for the 3-simplex. In [7] the null space dimensions for the 2-simplex are given by formulas for any degree d and for the 3-simplex they are tabulated up to degree 20.

The number of evaluation points in a particular integration rule is denoted by $F[\mathbf{K}]$, which is a linear function of the $K[\mathbf{n}]$:

$$F[\mathbf{K}] = \sum_{[\mathbf{n}]} v[\mathbf{n}] K[\mathbf{n}],$$

the sum being over all distinct classes $[\mathbf{n}]$. For an efficient numerical scheme, it is desirable to have F as small as possible. The absolute minimum for a given degree may, however, lead to negative or zero weights; suboptimal solutions therefore need to be considered as well. Also, there may be multiple solutions for given F .

The general problem of finding an optimal integration-rule structure can be formulated as the integer programming problem

$$\left\{ \begin{array}{l} \text{Minimise } F_i[\mathbf{K}] \text{ subject to} \\ \mathbf{K} \in \{\mathbf{K} \mid \mathbf{A}\mathbf{K} \leq -\mathbf{r}(d), \ F_i[\mathbf{K}] \geq F_{i-1} + 1\} \\ i = 1, 2, 3, \dots \end{array} \right.$$

The minimisation process may be started with $F_0 = -1$. The first absolute minimum F_1 is obtained for k_1 different structures \mathbf{K} denoted by $\mathbf{K} = \mathbf{K}_{11}, \mathbf{K}_{12}, \dots, \mathbf{K}_{1k_1}$. The second suboptimal minimum F_2 satisfying $F_2 \geq F_1 + 1$ is obtained for k_2 different structures denoted by $\mathbf{K} = \mathbf{K}_{21}, \mathbf{K}_{22}, \dots, \mathbf{K}_{2k_2}$, etc. In this way all successively weaker minima may be determined. In [9] the optimal rule structures and minima are listed up to the third minimum or the triangle, and in [8] they are listed up to the fifth minimum for the tetrahedron. To find rule structures that satisfy the conformity requirements and positivity of weights, the minimisation process had to be carried out to further minima. The minimisation problem has been tackled by simple enumeration, which took a considerable amount of computer time but was readily implemented in *Mathematica*.

Table 3.1 on page 416 in [7] contains some errors due to roundoff, which resulted in some incorrect rule structures listed in [8], see [11]. Table 4 in Appendix A is part of a corrected version of Table 3.1 in [7], provided by the author.

4. Construction of finite elements

Given the rule structures presented in the previous section, the next task is the set up and solve the corresponding nonlinear system of equations. In addition, some of the requirements listed at the end of Section 2, namely conformity and positivity of the integration weight, still have to be imposed. The conformity requirement provides additional constraints on the choice of polynomial basis functions, and hence on the consistency conditions. Positivity of the integration weights is checked after a nonlinear system has been solved.

4.1. TWO DIMENSIONS

The restriction of an M th degree polynomial to an edge of the triangle can be considered as the M th degree polynomial in a single variable on a finite interval, and is uniquely defined by $M + 1$ nodes on the edge, shared by the two triangles which meet at that edge. Here, the vertices of the triangle will be included as nodes. The nodal values elsewhere on the triangle have no effect on the continuity of the polynomial along the edge. Thus, to satisfy the continuity requirement, there should be $M + 1$ nodes on each edge. This corresponds to $3M$ nodes on the boundary of the element: 3 vertices and $M - 1$ nodes in the interior of each edge. This leaves $\frac{1}{2}(M + 1)(M + 2) - 3 - 3(M - 1) = \frac{1}{2}(M - 2)(M - 1)$ nodes for the interior of the triangle. A symmetric arrangement for the nodes is chosen, as described in Section 3. If for a certain arrangement of the nodes the weights are zero or negative, then additional nodes are inserted into the interior of the triangle. This increases the degree of the interpolating polynomials to M_f . Continuity can be maintained by requiring the restriction of these polynomials on the edges to be of degree M . This subspace of P_{M_f} is given by

$$\tilde{P}_{M_f} = \{p \in P_{M_f} \mid p|_{\mathbf{E}_k} \in P_M\},$$

where \mathbf{E}_k , ($k = 1, 2, 3$) are the edges of a triangle. This space can also be expressed as

$$\tilde{P}_{M_f} = P_M \oplus P_{M_f-3} * [b],$$

where $b = xy(1 - x - y)$ is the so-called bubble function, which vanishes on the boundary of the triangle. The number of nodes that uniquely defines a polynomial in this space is

$$3 + 3(M - 1) + \frac{1}{2}(M_f - 2)(M_f - 1). \quad (14)$$

The rule structure parameters can be expressed in terms of M and M_f as follows:

– number of nodes on the edges

$$3K[1] + 3K[2] + 6K[1, 1] = 3M, \quad (15)$$

– number of nodes in the interior of the triangle

$$K[3] + 3K[2, 1] + 6K[1, 1, 1] = \frac{1}{2}(M_f - 2)(M_f - 1), \quad (16)$$

where $M_f \geq M \geq 1$.

4.2. THREE DIMENSIONS

The restriction of an M th degree polynomial in three dimensions to one of the faces of a tetrahedron results in an M th degree polynomial in two variables, and is uniquely defined by $\frac{1}{2}(M+1)(M+2)$ nodes on the face, shared by two tetrahedra. Again, the vertices of the tetrahedron are included among the nodes. As in two dimensions the continuity requirement is satisfied if each face contains $\frac{1}{2}(M+1)(M+2)$ nodes. The polynomial is uniquely defined on the edges if there are $M+1$ nodes on each edge: 4 vertices and $M-1$ nodes in the interior of each. Therefore the total number of nodes on the boundary of the tetrahedron must equal $B = 4 + 6(M-1) + 4 \cdot \frac{1}{2}(M-2)(M-1)$. This leaves $\frac{1}{6}(M+3)(M+2)(M+1) - B = \frac{1}{6}(M-3)(M-2)(M-1)$ nodes for the interior of the tetrahedral volume. If for a certain arrangement of the nodes the weights are zero or negative then extra nodes are added to the tetrahedron. They can be inserted in the interior of the faces or the interior of the tetrahedron. Extra nodes on the faces increase the degree of the interpolating polynomial to M_f , having a restriction of degree M to the edges. Extra nodes in the interior of the tetrahedron increase the degree of the polynomial to M_i , which must have a restriction of degree M_f on the faces and a restriction of degree M on the edges in order to maintain continuity. The new polynomial space is

$$\tilde{P}_{M_i} = \{p \in P_{M_i} \mid p|_{\mathbf{F}_j} \in P_{M_f}, p|_{\mathbf{E}_k} \in P_M\},$$

where \mathbf{F}_j , ($j = 1, \dots, 4$), are the faces and \mathbf{E}_k , ($k = 1, \dots, 6$), the edges of a tetrahedron. This space can also be expressed as

$$\tilde{P}_{M_i} = P_M \oplus P_{M_f-3} * [b] \oplus \tilde{P}_{M_i-4} * [\tilde{b}],$$

where $\tilde{b} = xyz(1-x-y-z)$ is the bubble function, which vanishes on the boundary of the tetrahedron. The number of nodes that uniquely define a polynomial in this space is

$$4 + 6(M-1) + 4 \cdot \frac{1}{2}(M_f-2)(M_f-1) + \frac{1}{6}(M_i-3)(M_i-2)(M_i-1). \quad (17)$$

As for the triangle the three-dimensional rule structure parameters should satisfy additional conditions

– number of nodes on the edges

$$4K[1] + 6K[2] + 12K[1, 1] = 4 + 6(M-1), \quad (18)$$

– number of nodes in the interior of the faces

$$4K[3] + 12K[2, 1] + 24K[1, 1, 1] = 2(M_f-2)(M_f-1), \quad (19)$$

– number of nodes in the interior of the tetrahedron:

$$\begin{aligned} K[4] + 4K[3, 1] + 6K[2, 2] + 12K[2, 1, 1] + 24K[1, 1, 1, 1] \\ = \frac{1}{6}(M_i-3)(M_i-2)(M_i-1), \end{aligned} \quad (20)$$

where $M_i \geq M_f \geq M \geq 1$.

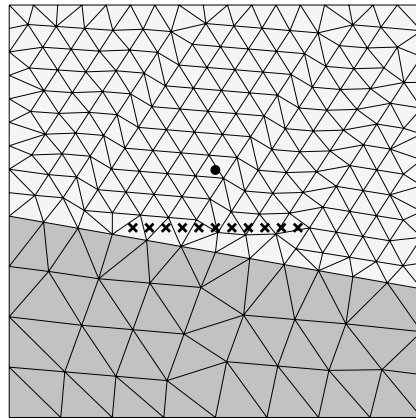


Figure 1. Example of a FEM grid for a simple reflection problem. The top layer has a velocity of 1.5 km/s, the bottom of 3.0 km/s. The source is marked by a dot, the receivers by crosses.

For a given integration degree the number of nodes is minimised subject to the consistency conditions, and the conformity conditions (15–16) for two dimensions and (18–20) for three dimensions, where M , M_f and M_i should be integer valued. Next, all optimal structures that result in the same minimum are determined. To find the following weaker minima, the process is repeated under the additional condition that the minimum is larger than the previous one, see Appendix A. In Appendix B the optimal rule structures for the triangle are tabulated up to degree 11, and for the tetrahedron, up to degree 8. Structures for which M is much smaller than M_f or M_f is much smaller than M_i are not tabulated.

The next step consists of fitting the moment equations (11) to obtain sufficiently accurate integration rules. In our case the rule should be of degree $q = M + M_f - 2$, in two dimensions, and $q = M + M_i - 2$, in three dimensions, for given values of M , M_f and M_i to obtain the same order of accuracy as without mass lumping, see *e.g.* [12, 13]. The systems were solved using *Mathematica*, and the more complicated ones were solved numerically using the HYBRD routine of the MINPACK library.

Following this approach all known and a number of new elements have been found, see Appendix C. In two dimensions elements up to sixth order ($M = 5$) have been found, with the ones of sixth order being new. Three-dimensional elements have been found up to fourth order ($M = 3$), with the one of fourth order being new. The lower-order elements can also be found in [4, 5].

5. Efficiency of triangular elements

A comparison between finite differences and higher-order finite elements has been carried out in [5] for a simple reflection problem. It was shown that the finite-difference method is less efficient than the finite-element method, despite the added complexity of the latter. The main reason is that the high-order finite-difference method loses its accuracy near sharp interfaces in the velocity model. Finite elements with edges that fit the interface maintain their accuracy.

Among the elements of various order, it turned out that higher-order elements are more efficient than the lower-order ones, at least up to fifth order. Here we extend the results of [5] by including the new sixth-order element ($M = 5$). The main questions are: which temporal error is the most efficient for a given spatial error, and which spatial error is the most efficient?

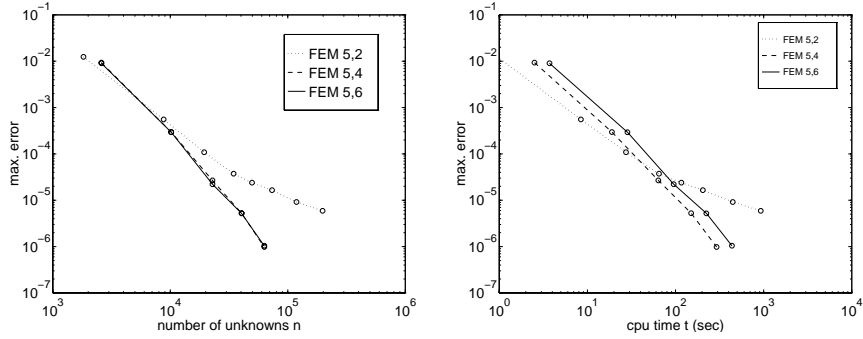


Figure 2. Errors for the FEM (6th order in space) as a function of the number of degrees of freedom (left) and cpu-time (right) using a 2nd, 4th, and 6th order time-stepping scheme.

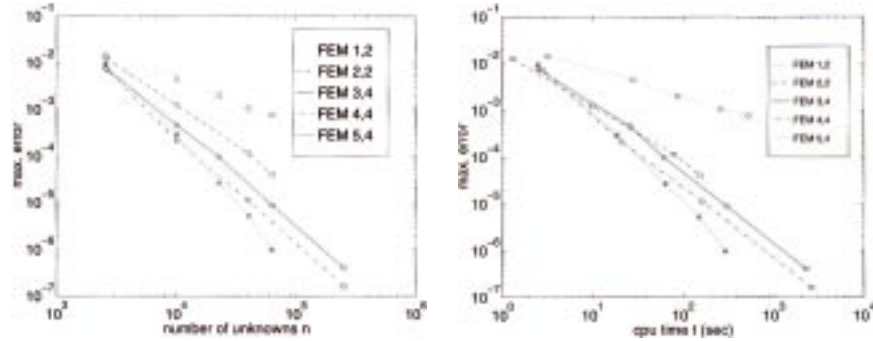


Figure 3. Comparison of various orders.

Figure 1 shows the simple two-dimensional reflection problem and a finite-element grid that follows the sharp interface. The size of the domain is $1000 \times 1000 \text{ m}^2$. The grid density has been scaled to the velocity $c(\mathbf{x})$, which is 1.5 km/s in the upper and 3.0 km/s in the lower part. The source term $f(\mathbf{x})$ is set of zero; instead, the computation is initialised with the exact solution of a point source at $t_0 = 0.1 \text{ s}$, at which time the direct wave has not yet reached the interface, *i.e.*, $u(t_0 \mathbf{x})$ and $u_t(t_0 \mathbf{x})$ are given as the exact response of a point source firing around $t = 0$ with a given wavelet. The traces (receiver data) have been recorded at the positions marked by crosses in Figure 1. For simplicity, zero Dirichlet boundary conditions

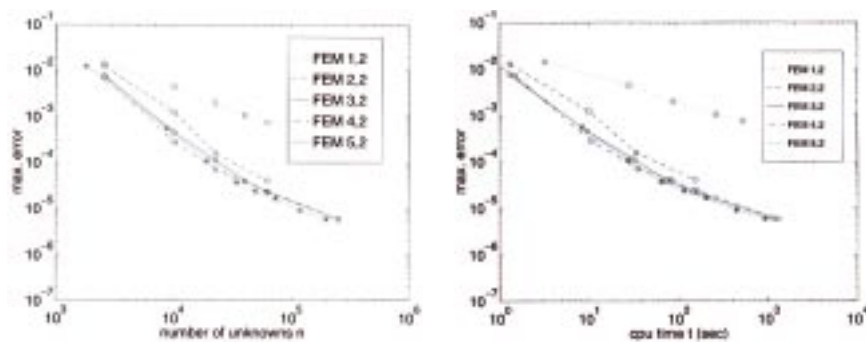


Figure 4. Comparison of various orders with 2nd-order time-stepping.

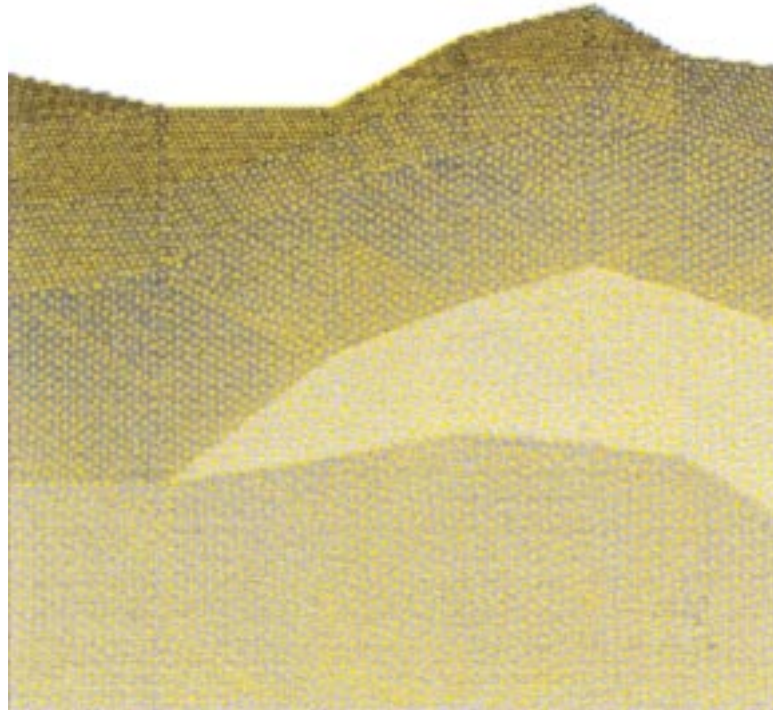


Figure 5. Triangulated subsurface velocity model.

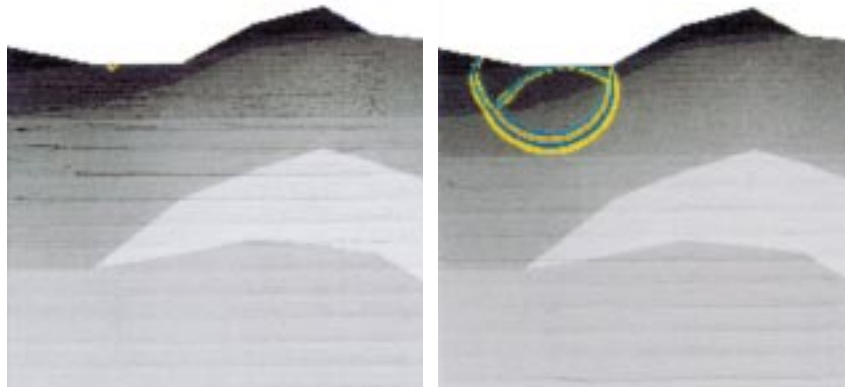


Figure 6. Initial shot (left) and snapshots at 0.5 seconds (right).

have been used and the computation has been stopped before reflections off the boundaries reached the receivers.

We have compared the numerical solution to the exact solution for this simple problem, using trace data between 0.102 and 0.300 seconds at 2 ms intervals.

Figure 2 shows the maximum error as a function of the number of degrees of freedom and cpu-time, respectively. The computations were carried out on an IBM RS/6000 3AT with a program written in C, using double precision arithmetic. The time-stepping scheme is the same as in [10]. Here second, fourth, and sixth order in time are considered. The time-step Δt was chosen somewhat arbitrarily such that $\Delta t \sqrt{n} \sim 0.022$, which honoured the stability limit; here n is the number of unknowns.

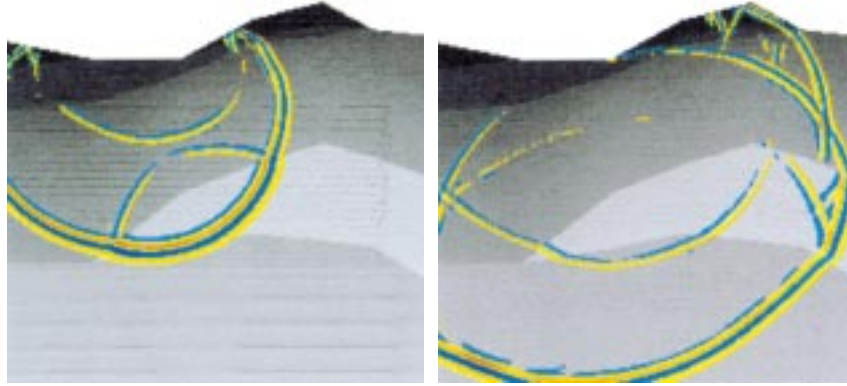


Figure 7. Snapshots at 1.0 (left) and 1.5 seconds (right).

From the left panel of Figure 2 it can be deduced from the slope of the line through the measured points that the scheme behaves as a sixth-order scheme for the larger errors. For smaller errors, the temporal error of the second-order time-stepping scheme starts to show up. For the fourth- and sixth-order time-stepping scheme, the errors are practically the same, showing that in those cases the spatial error dominates. Because the sixth-order time-stepping scheme involves about 1.5 times more operations than the fourth-order scheme, it appears as the less efficient one in the right panel of Figure 2. For larger values of the error, the second-order time-stepping scheme is more efficient.

Next, a comparison among various orders ($M = 1, \dots, 5$) was made. For each order, the time-stepping scheme was chosen that appears to be the most efficient at the level of a maximum error around 10^{-5} (for the present problem, 1 percent accuracy corresponds to an error between 10^{-4} and 10^{-3}). The results are summarised in Figure 3. The results for second-order time-stepping are displayed in Figure 4. These figures show that for moderate accuracy (10^{-4} or somewhat larger), fourth-order in space and second-order in time is attractive. For high accuracy, sixth-order in space and fourth-order in time becomes the more efficient scheme.

This still leaves the question open, whether or not it pays to go to schemes of still higher spatial order. Note that efficiency is here discussed on the basis of cpu-time. If the size of available memory is a bottleneck – which it may be for realistic three-dimensional computations – higher order schemes can provide the same accuracy as lower order schemes but with less storage requirements.

6. Seismic example

A practical example of a seismic shot in a hilly area is shown in Figure 5. The width is 6 km, the depth 5 km, and the highest surface point is 550 m. Computations were carried out with a fourth-order scheme, both in space and time. The background velocity model is drawn in grey; lighter shades correspond to higher velocities. The velocity ranges from 1700 km/s near the surface to 4000 km/s at larger depths, and are constant or slowly varying inside the various geological layers. The firing of the initial shot and snapshots at later times are shown in Figures 6 and 7.

7. Conclusions

A systematic approach for the construction of mass-lumped triangular and tetrahedral elements for solving the wave equation has been presented. The search has been restricted to elements that fulfill the following requirements: (i) conformity, (ii) symmetric arrangement of nodes, (iii) positive integration weights, (iv) same order of accuracy as elements without mass lumping. Using the theory of consistency conditions, we reproduced all known lower-order elements. A new sixth-order triangular element and a new fourth-order tetrahedral element have been found.

The computational efficiency of the new sixth-order triangular element has been tested by consideration of a simple two-dimensional seismic reflection problem. For this problem, it proved to be more efficient (with fourth-order time-stepping) than the lower-order elements if high accuracy is desired. For moderate accuracy, fourth-order in space and second-order in time appears to be sufficient, at least for the simple short-time reflection problem considered here. The question remains if elements of still higher accuracy will be even more efficient when high accuracy is a requirement.

The efficiency of the mass-lumped tetrahedral elements is unknown, both in comparison to the finite-difference method, and in comparison to standard tetrahedral elements of higher order. In the last case, the use of fast iterative sparse-matrix solvers may produce a scheme that competes with the rather complex mass-lumped elements.

The use of the consistency conditions helped in the search for new elements, but the conditions are no guarantee for existence and uniqueness. Other elements may exist that do not obey these conditions, although this is expected to be unlikely. Even when the consistency conditions are applied to select promising candidate nonlinear systems, the actual solution of these systems remains difficult and has only been accomplished for some of the candidates listed in Appendix B.

Other outstanding problems are the choice of absorbing boundary conditions and the extension to acoustic and elastic equations.

Appendix

A. Integer programming problem

A.1. TWO DIMENSIONS

The function to be minimised is

$$F_i[\mathbf{K}] = 3K[1] + 3K[2] + 6K[1, 1] + K[3] + 3K[2, 1] + 6K[1, 1, 1] \quad (21)$$

subject to

$$\begin{aligned} \mathbf{AK} &\leq -\mathbf{r}(d), & F_i[\mathbf{K}] &\geq F_{i-1} + 1, & i &= 1, 2, 3 \dots, & F_0 &= -1, \\ 3K[1] + 3K[2] + 6K[1, 1] &= 3M, & K[3] + 3K[2, 1] + 6K[1, 1, 1] &= \frac{1}{2}(M_f - 2)(M_f - 1), \end{aligned}$$

Table 3. The columns below show each value of d (the degree of the integration rule) represents the vector $\mathbf{r}(d)$ (containing the dimensions of null space intersections in two dimensions).

Degree d of integration rule														
1	2	3	4	5	6	7	8	9	10	11	12	13	14	
-1	-1	-1	-1	-1	-1	-1	-1	-1	-1	-1	-1	-1	-1	
-1	-1	-1	-1	-1	-1	-1	-1	-1	-1	-1	-1	-1	-1	
-1	-1	-1	-1	-1	-1	-1	-1	-1	-1	-1	-1	-1	-1	
1	2	3	4	5	7	8	10	12	14	16	19	21	24	
0	0	1	1	2	3	4	5	7	8	10	12	14	16	
0	0	0	0	0	1	1	2	3	4	5	7	8	10	
0	0	0	0	0	0	0	0	1	1	2	3	4	5	

where

$$\mathbf{A} = \begin{pmatrix} 1 & 0 & 0 & 0 & 0 & 0 \\ 0 & 1 & 0 & 0 & 0 & 0 \\ 0 & 0 & 0 & 1 & 0 & 0 \\ -1 & -1 & -2 & -1 & -2 & -3 \\ 0 & 0 & 0 & -1 & -2 & -3 \\ 0 & 0 & -2 & 0 & 0 & -3 \\ 0 & 0 & 0 & 0 & 0 & -3 \end{pmatrix}, \quad (22)$$

and $\mathbf{r}(d)$ is a column vector given in Table 3.

A.2. THREE DIMENSIONS

The function to be minimised is

$$\begin{aligned} F_i[\mathbf{K}] = & 4K[1] + 6K[2] + 12K[1, 1] + 4K[3] + 12K[2, 1] + 24K[1, 1, 1] \\ & + K[4] + 4K[3, 1] + 6K[2, 2] + 12K[2, 1, 1] + 24K[1, 1, 1, 1] \end{aligned} \quad (23)$$

subject to

$$\begin{aligned} \mathbf{A}\mathbf{K} \leq -\mathbf{r}(d), \quad F_i[\mathbf{K}] \geq F_{i-1} + 1, \quad i = 1, 2, 3 \dots, \quad F_0 = -1, \\ 4K[1] + 6K[2] + 12K[1, 1] = 4 + 6(M - 1), \\ 4K[3] + 12K[2, 1] + 24K[1, 1, 1] = 2(M_f - 2)(M_f - 1), \\ K[4] + 4K[3, 1] + 6K[2, 2] + 12K[2, 1, 1] + 24K[1, 1, 1, 1] = \frac{1}{6}(M_i - 3)(M_i - 2)(M_i - 1), \end{aligned}$$

where

$$\mathbf{A} = \begin{pmatrix} 1 & 0 & 0 & 0 & 0 & 0 & 0 & 0 & 0 & 0 & 0 \\ 0 & 1 & 0 & 0 & 0 & 0 & 0 & 0 & 0 & 0 & 0 \\ 0 & 0 & 0 & 1 & 0 & 0 & 0 & 0 & 0 & 0 & 0 \\ 0 & 0 & 0 & 0 & 0 & 0 & 1 & 0 & 0 & 0 & 0 \\ -1 & -1 & -2 & -1 & -2 & -3 & -1 & -2 & -2 & -3 & -4 \\ 0 & 0 & 0 & -1 & -2 & -3 & -1 & -2 & -2 & -3 & -4 \\ 0 & 0 & -2 & 0 & 0 & -3 & -1 & -2 & -2 & -3 & -4 \\ 0 & 0 & 0 & 0 & 0 & 0 & -1 & -2 & -2 & -3 & -4 \\ 0 & -1 & -2 & 0 & -2 & -3 & 0 & 0 & -2 & -3 & -4 \\ -1 & 0 & -2 & -1 & -2 & -3 & 0 & -2 & 0 & -3 & -4 \\ 0 & 0 & 0 & 0 & 0 & -3 & 0 & 0 & 0 & 0 & -4 \\ 0 & 0 & 0 & 0 & 0 & -3 & -1 & -2 & -2 & -3 & -4 \\ 0 & 0 & 0 & 0 & -2 & -3 & 0 & 0 & -2 & -3 & -4 \\ 0 & 0 & 0 & -1 & -2 & -3 & 0 & -2 & 0 & -3 & -4 \\ 0 & 0 & -2 & 0 & 0 & -3 & 0 & 0 & -2 & -3 & -4 \\ 0 & 0 & -2 & 0 & 0 & -3 & 0 & -2 & 0 & -3 & -4 \\ 0 & 0 & 0 & 0 & 0 & 0 & 0 & 0 & -2 & -3 & -4 \\ 0 & 0 & 0 & 0 & 0 & 0 & 0 & -2 & 0 & -3 & -4 \\ 0 & 0 & 0 & 0 & 0 & 0 & 0 & 0 & 0 & 0 & -4 \\ 0 & 0 & -2 & 0 & -2 & -3 & 0 & 0 & 0 & 0 & -4 \\ 0 & 0 & 0 & 0 & -2 & -3 & 0 & 0 & 0 & 0 & -4 \\ 0 & 0 & 0 & 0 & -2 & -3 & 0 & 0 & 0 & 0 & -4 \\ 0 & 0 & 0 & 0 & 0 & 0 & 0 & 0 & 0 & 0 & -4 \end{pmatrix}, \quad (24)$$

and $\mathbf{r}(d)$ is a column vector given in Table 4.

B. Rule structures

In this appendix the consistent rule structures that were obtained from the minimisation problem in Appendix A are tabulated. The two-dimensional structures are tabulated up to degree 11 in Table 5; they are described by 11 integers

$$d, N, K_1, \dots, K_6, M, M_f, q,$$

and the three-dimensional structures are tabulated up to degree 8 in Table 6, described by 17 integers

$$d, N, K_1, \dots, K_{11}, M, M_f, M_i, q,$$

where

- d = actual degree of the integration rule,
- N = number of nodes,
- K_i = structure parameter,
- M, M_f, M_i = degrees of interpolating polynomials (see Section 4),
- q = required degree of the integration rule ($q \leq d$).

Table 4. The columns below each value of d (the degree of the integration rule) represents the vector $\mathbf{r}(d)$ (containing the dimensions of null space intersections in three dimensions).

Degree d of integration rule												
1	2	3	4	5	6	7	8	9	10	11	12	
-1	-1	-1	-1	-1	-1	-1	-1	-1	-1	-1	-1	
-1	-1	-1	-1	-1	-1	-1	-1	-1	-1	-1	-1	
-1	-1	-1	-1	-1	-1	-1	-1	-1	-1	-1	-1	
-1	-1	-1	-1	-1	-1	-1	-1	-1	-1	-1	-1	
1	2	3	5	6	9	11	15	18	23	27	34	
0	0	1	2	3	5	7	10	13	17	21	27	
0	0	0	1	1	3	4	7	9	13	16	22	
0	0	0	1	1	2	3	5	6	9	11	15	
0	0	0	1	1	3	4	7	9	13	16	22	
0	0	1	2	3	5	7	10	13	17	21	27	
0	0	0	0	0	0	0	0	0	0	0	0	
0	0	0	1	1	2	3	5	7	10	13	18	
0	0	0	0	0	1	2	4	6	9	12	17	
0	0	0	0	1	2	4	6	9	12	16	21	
0	0	0	0	0	0	0	2	3	6	8	13	
0	0	0	0	0	1	2	4	6	9	12	17	
0	0	0	0	0	0	0	1	1	3	4	7	
0	0	0	0	0	0	1	2	3	5	7	10	
0	0	0	0	0	0	0	0	0	0	0	0	
0	0	0	0	0	1	2	4	6	9	12	17	
0	0	0	0	0	0	0	1	2	4	6	10	
0	0	0	0	0	0	1	2	4	6	9	13	
0	0	0	0	0	0	1	2	4	6	9	13	
0	0	0	0	0	0	0	1	2	1	6	10	
0	0	0	0	0	0	0	0	0	1	2	4	
0	0	0	0	0	0	0	0	1	2	4	7	

For some structures additional information is given in the last column. Structures for which there is a solution with positive weights are indicated by xpw , where x denotes the number of solutions that has been found. Structures for which there is a solution with one or more negative weights are indicated by xnw . If there is at least one zero weight, this is indicated by xzw . An asterisk * means that the solution is given in Appendix C. If no indication is given at all, it means we have not been able to find a solution but one still might exist.

C. Results

For each element the nodes are listed in one table (See Tables 7–25). On each line one node is given, followed by the number of symmetric nodes, the corresponding weight and parameter(s).

Table 5. Two-dimensional structures of degrees 1 to 11.

d	N	K_1	K_2	K_3	K_4	K_5	K_6	M	M_f	q	
1	3	1	0	0	0	0	0	1	1	0	1 pw*
2	6	1	1	0	0	0	0	2	2	2	1 zw
3	7	1	1	0	1	0	0	2	3	3	1 pw*
4	9	1	1	0	0	1	0	2	4	4	1 pw
4	10	1	0	1	1	0	0	3	3	4	1 nw
5	12	1	1	0	0	0	1	2	5	5	
5	12	1	1	0	0	2	0	2	5	5	
5	12	1	0	1	0	1	0	3	4	5	1 pw*
6	15	1	0	1	0	2	0	3	5	6	
7	18	1	1	1	0	2	0	4	5	7	1 pw*
7	19	1	0	1	1	1	1	3	6	7	
7	19	1	0	1	1	3	0	3	6	7	
8	19	1	0	1	1	3	0	3	6	7	
8	22	1	1	1	1	1	1	4	6	8	1 nw
8	22	1	1	1	1	3	0	4	6	8	
8	24	1	0	1	0	1	2	3	7	8	3 pw
8	24	1	0	1	0	3	1	3	7	8	
8	24	1	0	1	0	5	0	3	7	8	
9	24	1	0	1	0	3	1	3	7	8	
9	27	1	1	1	0	1	2	4	7	9	1 pw*
9	27	1	1	1	0	3	1	4	7	9	3 pw
10	30	1	0	2	0	3	1	5	7	10	1 pw*
10	33	1	1	1	0	1	3	4	8	10	3 pw
10	33	1	1	1	0	3	2	4	8	10	
10	33	1	1	1	0	5	1	4	8	10	
11	33	1	1	1	0	3	2	4	8	10	
11	33	1	1	1	0	5	1	4	8	10	
11	36	1	0	2	0	1	3	5	8	11	2 pw*
11	36	1	0	2	0	3	2	5	8	11	6 pw*
11	36	1	0	2	0	5	1	5	8	11	

Table 6. Three-dimensional structures of degrees 1 to 8.

d	N	K_1	K_2	K_3	K_4	K_5	K_6	K_7	K_8	K_9	K_{10}	K_{11}	M	M_f	M_i	q	
1	4	1	0	0	0	0	0	0	0	0	0	0	1	1	1	0	1 pw*
2	10	1	1	0	0	0	0	0	0	0	0	0	2	2	2	2	1 nw
3	14	1	1	0	1	0	0	0	0	0	0	0	2	3	3	3	1 zw
4	23	1	1	0	0	1	0	1	0	0	0	0	2	4	4	4	1 pw*
5	26	1	1	0	0	1	0	0	1	0	0	0	2	4	5	5	
5	29	1	0	1	0	1	0	1	0	0	0	0	3	4	4	5	
5	38	1	1	0	0	0	1	0	1	0	0	0	2	5	5	5	
5	38	1	1	0	0	2	0	0	1	0	0	0	2	5	5	5	
6	44	1	1	0	0	0	1	0	1	1	0	0	2	5	6	6	
6	44	1	1	0	0	2	0	0	1	1	0	0	2	5	6	6	
6	44	1	0	1	0	2	0	0	1	0	0	0	3	5	5	6	
7	42	1	1	0	0	1	0	0	2	0	1	0	2	4	7	7	
7	42	1	1	0	0	1	0	0	2	2	0	0	2	4	7	7	
7	50	1	0	1	0	2	0	0	1	1	0	0	3	5	6	7	2 pw*, 1 nw*
7	66	1	0	1	1	1	1	0	1	1	0	0	3	6	6	7	
7	66	1	0	1	1	3	0	0	1	1	0	0	3	6	6	7	
8	60	1	0	1	0	2	0	0	2	2	0	0	3	5	7	8	
8	76	1	0	1	1	1	1	0	2	0	1	0	3	6	7	8	
8	76	1	0	1	1	1	1	0	2	2	0	0	3	6	7	8	
8	76	1	0	1	1	3	0	0	2	0	1	0	3	6	7	8	
8	76	1	0	1	1	3	0	0	2	2	0	0	3	6	7	8	

C.1. REVIEW OF KNOWN ELEMENTS

Table 7. The standard second-order triangular element ($M = M_f = d = 1$).

Nodes	Weights	Parameters
(0, 0)	3 $\frac{1}{6}$	—

Table 9. A fourth-order triangular element ($M = 3$, $M_f = 4$, $d = 5$).

Nodes	Weights	Parameters
(0, 0)	3 $\frac{1}{90} - \frac{\sqrt{7}}{720}$	—
$(\alpha, 0)$	6 $\frac{7}{720} + \frac{\sqrt{7}}{180}$	$\frac{1}{2} - \frac{\sqrt{441-84(7-\sqrt{7})}}{42}$
(β, β)	3 $\frac{49}{360} - \frac{7\sqrt{7}}{720}$	$\frac{1}{3}(1 - \frac{1}{\sqrt{7}})$

Table 8. A third-order triangular element ($M = 2$, $M_f = 3$, $d = 3$).

Nodes	Weights	Parameters
(0, 0)	3 $\frac{1}{40}$	—
$(\frac{1}{2}, 0)$	3 $\frac{1}{15}$	—
$(\frac{1}{3}, \frac{1}{3})$	1 $\frac{9}{40}$	—

Table 10. A fifth-order triangular element with 18 nodes for $\mathbf{K} = (1, 1, 1, 0, 2, 0)$ ($M = 4$, $M_f = 5$, $d = 7$).

Nodes	Weights	Parameters
(0, 0)	3 $\frac{1}{315}$	—
$(\frac{1}{2}, 0)$	3 $\frac{4}{315}$	—
$(\alpha, 0)$	6 $\frac{3}{280}$	$\frac{1}{2}(1 - \frac{1}{\sqrt{3}})$
(β_1, β_1)	3 $\frac{163}{2520} + \frac{47\sqrt{7}}{8820}$	$\frac{5+\sqrt{7}}{18}$
(β_2, β_2)	3 $\frac{163}{2520} - \frac{47\sqrt{7}}{8820}$	$\frac{5-\sqrt{7}}{18}$

Table 11. A fifth-order triangular element with 27 nodes for $\mathbf{K} = (1, 1, 1, 0, 1, 2)$ ($M = 4$, $M_f = 7$, $d = 9$).

Nodes	Weights	Parameters
(0, 0)	3 $0.7425845258035245\text{E-03}$	—
$(\frac{1}{2}, 0)$	3 $0.5228925775971095\text{E-03}$	—
$(\alpha, 0)$	6 $0.5780744536385346\text{E-02}$	$0.1044413784858067\text{E-00}$
(β, β)	3 $0.3143086701106134\text{E-01}$	$0.1124612712776796\text{E-00}$
(γ_1, δ_1)	6 $0.2670516378072029\text{E-01}$	$0.3964634972921077\text{E-01}$
		$0.3373407414205641\text{E-00}$
(γ_2, δ_2)	6 $0.3449925295899670\text{E-01}$	$0.1868572380229495\text{E-00}$
		$0.3156575833835992\text{E-00}$

Table 12. The standard second-order tetrahedral element ($M = M_f = M_i = d = 1$).

Nodes	Weights	Parameters
(0, 0, 0)	4 $\frac{1}{24}$	—

Table 13. A third-order tetrahedral element ($M = 2$, $M_f = M_i = d = 4$).

Nodes	Weights	Parameters
(0, 0, 0)	4 $\frac{13-3\sqrt{13}}{10080}$	—
$(\frac{1}{2}, 0, 0)$	6 $\frac{4-\sqrt{13}}{315}$	—
$(\alpha, \alpha, 0)$	12 $\frac{29+17\sqrt{13}}{10080}$	$\frac{7-\sqrt{13}}{18}$
$(\frac{1}{4}, \frac{1}{4}, \frac{1}{4})$	1 $\frac{16}{315}$	—

C.2. NEW TRIANGULAR ELEMENTS

Table 14. A sixth-order triangular element with 30 nodes ($M = 5$, $M_f = 7$, $d = 10$).

Nodes	Weights	Parameters
(0, 0)	3	0.7094239706792450E-03
($\alpha_1, 0$)	6	0.6190565003676629E-02
($\alpha_2, 0$)	6	0.3480578640489211E-02
(β_1, β_1)	3	0.3453043037728279E-01
(β_2, β_2)	3	0.4590123763076286E-01
(β_3, β_3)	3	0.1162613545961757E-01
(γ_1, δ_1)	6	0.2727857596999626E-01
		0.7819258362551702E-01
		0.2210012187598900E-00

Table 16. A second sixth-order triangular element of the same type.

Nodes	Weights	Parameters
(0, 0)	3	0.4583058548765858E-03
($\alpha_1, 0$)	6	0.4697276305236619E-02
($\alpha_2, 0$)	6	0.3367070457223120E-02
(β_1, β_1)	3	0.2849177084300189E-01
(β_2, β_2)	3	0.8948103929621387E-02
(β_3, β_3)	3	0.3275210436109946E-01
(γ_1, δ_1)	6	0.2135074610440116E-01
		0.3686932305165343E-00
(γ_2, δ_2)	6	0.1859309797217277E-01
		0.7474371355107266E-00
		0.1845656598467499E-00

Table 18. A fourth sixth-order triangular element of the same type.

Nodes	Weights	Parameters
(0, 0)	3	0.6977749977819948E-03
($\alpha_1, 0$)	6	0.2929845918662817E-02
($\alpha_2, 0$)	6	0.5039500082674611E-02
(β_1, β_1)	3	0.2457088105214646E-01
(β_2, β_2)	3	0.2972585619925110E-01
(β_3, β_3)	3	0.1178089444287955E-01
(γ_1, δ_1)	6	0.205239905209480E-01
		0.6856705032286132E-01
		0.2129399133002941E-00
(γ_2, δ_2)	6	0.2145229339387155E-01
		0.566808553115408E-00
		0.1535990892761941E-00

Table 20. A sixth sixth-order triangular element of the same type.

Nodes	Weights	Parameters
(0, 0)	3	0.4762675286979898E-03
($\alpha_1, 0$)	6	0.2897841311190826E-02
($\alpha_2, 0$)	6	0.4491124346734268E-02
(β_1, β_1)	3	0.3517078577575594E-01
(β_2, β_2)	3	0.1350590535760379E-01
(β_3, β_3)	3	0.2387982403384744E-01
(γ_1, δ_1)	6	0.2498014209662454E-01
		0.2645456108709536E-00
		0.1360625094869939E-00
(γ_2, δ_2)	6	0.1444783420383112E-01
		0.1360625094869939E-00
		0.5194908177061736E-01

Table 15. A sixth-order triangular element with 36 nodes for $\mathbf{K} = (1, 0, 2, 0, 3, 2)$ ($M = 5$, $M_f = 8$, $d = 11$).

Nodes	Weights	Parameters
(0, 0)	3	0.6082563295533433E-03
($\alpha_1, 0$)	6	0.486255131214688E-02
($\alpha_2, 0$)	6	0.2877488812209360E-02
(β_1, β_1)	3	0.2423831099156024E-01
(β_2, β_2)	3	0.1229878329128456E-01
(β_3, β_3)	3	0.3302578307250388E-01
(γ_1, δ_1)	6	0.1754479406987699E-01
		0.7265336385659892E-00
		0.2115723052694821E-00
(γ_2, δ_2)	6	0.2296293229758128E-01
		0.5850352547280820E-00
		0.1437555396489239E-00

Table 17. A third sixth-order triangular element of the same type.

Nodes	Weights	Parameters
(0, 0)	3	0.6582643475372946E-03
($\alpha_1, 0$)	6	0.2887997749452224E-02
($\alpha_2, 0$)	6	0.4963909456272002E-02
(β_1, β_1)	3	0.3153470767800203E-01
(β_2, β_2)	3	0.119547103823643E-01
(β_3, β_3)	3	0.2438923490441436E-01
(γ_1, δ_1)	6	0.1905592143754818E-01
		0.6549274992240129E-01
(γ_2, δ_2)	6	0.2215666570601087E-01
		0.1482693720952231E-00
		0.2753149271480059E-00

Table 19. A fifth sixth-order triangular element of the same type.

Nodes	Weights	Parameters
(0, 0)	3	0.7843097667098473E-03
($\alpha_1, 0$)	6	0.5360806770285871E-02
($\alpha_2, 0$)	6	0.3612423945705114E-02
(β_1, β_1)	3	0.2935538218715718E-01
(β_2, β_2)	3	0.1259016943796081E-01
(β_3, β_3)	3	0.2477162854391181E-01
(γ_1, δ_1)	6	0.2637983755607086E-01
		0.7938836834591467E-01
		0.2240733927557592E-00
(γ_2, δ_2)	6	0.1422952009340166E-01
		0.4365216866929358E-00
		0.4976858328596177E-00

Table 21. A sixth-order triangular element with 36 nodes for $\mathbf{K} = (1, 0, 2, 0, 1, 3)$ ($M = 5$, $M_f = 8$, $d = 11$).

Nodes	Weights	Parameters
(0, 0)	3	0.1203429728164228E-03
($\alpha_1, 0$)	6	0.5648070482775567E-02
($\alpha_2, 0$)	6	0.1434742885973307E-02
(β, β)	3	0.2450479451803485E-01
(γ_1, δ_1)	3	0.2591187746397450E-01
		0.4673667678466049E-00
(γ_2, δ_2)	3	0.1112690810816592E-01
		0.3635254452027588E-01
(γ_3, δ_3)	6	0.2689907564701840E-01
		0.1150656775801793E-00
		0.2381461891158076E-00
		0.9531342890758771E-01

Table 22. A second sixth-order triangular element of the same type.

Nodes	Weights	Parameters
(0, 0)	3	0.7892941754415492E-03
($\alpha_1, 0$)	6	0.2438106746957435E-02
($\alpha_2, 0$)	6	0.5477346210172896E-02
(β, β)	3	0.2656035113426609E-01
(γ_1, δ_1)	3	0.2721390945227405E-01
		0.8454313312796995E-01
(γ_2, δ_2)	3	0.7684436539507441E-02
		0.8481558435195644E-01
(γ_3, δ_3)	6	0.2684471172956770E-01
		0.3148364616424038E-00
		0.4785704481357608E-00

C.3. TETRAHEDRAL ELEMENTS

Table 23. A fourth-order tetrahedral element with 50 nodes ($M = 3$, $M_f = 5$, $M_i = 6$, $d = 7$).

Nodes	Weights	Parameters
(0, 0, 0)	4	0.2143608668049743E-03
(α , 0, 0)	12	0.8268179517797114E-03
(β_1 , β_1 , 0)	12	0.1840177904191860E-02
(β_2 , β_2 , 0)	12	0.1831324329245650E-02
(γ , γ , γ)	4	0.7542468904648131E-02
(δ , δ , $\frac{1}{2} - \delta$)	6	0.1360991755970793E-01
		0.1252462362578136E-00

Table 24. A second fourth-order tetrahedral element with 50 nodes ($M = 3$, $M_f = 5$, $M_i = 6$, $d = 7$).

Nodes	Weights	Parameters
(0, 0, 0)	4	0.2321968872348930E-03
(α , 0, 0)	12	0.7328680241632055E-03
(β_1 , β_1 , 0)	12	0.2529792598144742E-02
(β_2 , β_2 , 0)	12	0.1564461923378417E-02
(γ , γ , γ)	4	0.7127911446564579E-02
(δ , δ , $\frac{1}{2} - \delta$)	6	0.1321679379720540E-01
		0.1258796196682507E-00

Table 25. A fourth-order tetrahedral element with negative weights ($M = 3$, $M_f = 5$, $M_i = 6$, $d = 7$).

Nodes	Weights	Parameters
(0, 0, 0)	4	-0.1154427535224906E-02
(α , 0, 0)	12	0.2601367173696685E-02
(β_1 , β_1 , 0)	12	0.5976671540633744E-02
(β_2 , β_2 , 0)	12	-0.1463055009746034E-01
(γ , γ , γ)	4	0.3835587013796648E-01
(δ , δ , $\frac{1}{2} - \delta$)	6	0.1508183880887654E-01
		0.3785672017136074E-00

Acknowledgements. The authors are indebted to Michel Kern of INRIA Rocquencourt for pointing us to Keast's papers, and to Patrick Keast for sending the corrected tables.

References

1. I. Fried and D. S. Malkus, Finite element mass matrix lumping by numerical integration without convergence rate loss. *Int. J. Solids Struc.* 11 (1976) 461–466.
2. G. Cohen, P. Joly and N. Tordjman, Construction and analysis of higher order finite elements with mass lumping for the wave equation. In: R. Kleinman, T. Angell, D. Colton, F. Santosa and I. Stakgold (eds), *Proc. of the 2nd International Conference on Mathematical and Numerical Aspects of Wave Propagation*. Philadelphia: SIAM (1993) pp. 152–160.
3. G. Cohen, P. Joly and N. Tordjman, Higher order triangular finite elements with mass lumping for the wave equation. In: G. Cohen, E. Bécache, P. Joly and J. E. Roberts (eds), *Proc. of the 3rd International Conference on Mathematical and Numerical Aspects of Wave Propagation*. Philadelphia: SIAM (1995) pp. 270–279.
4. N. Tordjman, Éléments finis d'ordre élevé avec condensation de masse pour l'équation des ondes. Ph.D. dissertation, L'Université Paris IX Dauphine (1995) 300 pp.
5. W. A. Mulder, A comparison between higher-order finite elements and finite differences for solving the wave equation, In: J.-A. Désidéri, P. Le Tallec, E. Oñate, J. Périaux and E. Stein (eds), *Proceedings of the Second ECCOMAS Conference on Numerical Methods in Engineering* (Paris, Sept. 9–13, 1996), John Wiley and Sons (1996) pp. 344–350.
6. W. A. Mulder, Spurious modes in finite-element discretisations of the wave equation may not be all that bad. Submitted to *Appl. Num. Math.*
7. P. Keast and J. C. Diaz, Fully symmetric integration formulas for the surface of the sphere in s dimensions. *SIAM J. Num. Anal.* 20 (1983) 406–419.
8. P. Keast, Moderate-degree tetrahedral quadrature formulas. *Comp. Meth. Appl. Mech. Eng.* 55 (1986) 339–348.
9. P. Keast, Cubature formulas for the surface of the sphere. *J. Comp. Appl. Math.* 17 (1987) 151–172.
10. M. A. Dablain, The application of higher-order differencing to the scalar wave equation. *Geophysics* 51 (1986) 54–66.
11. J. I. Maeztu and E. Sainz de la Maza, Consistent structures of invariant quadrature rules for the n -Simplex. *Math. Comp.* 64 (1995) 1171–1192.
12. P. G. Ciarlet and J. L. Lions, *Handbook of Numerical Analysis. Vol. II: Finite Element Methods. (Part 1)*. Amsterdam: North-Holland (1989) 928 pp.
13. G. Strang and G. J. Fix, *An Analysis of the Finite Element Method*. Englewood Cliffs, N.J.: Prentice Hall (1973) 306 pp.